Nonlinear fiber Optics: Fundamentals & Applications

Thibaut Sylvestre

Department of Optics, FEMTO-ST institute, CNRS
University of Franche-Comté, Besançon, France.

Nonlinear optical effects are remarkable physical phenomena that can occur when a high-intensity light beam propagates through an optical medium [1]. If the pump beam is intense enough and the medium exhibits the suitable nonlinear behavior, the typical properties of the medium (absorption, refractive index) can alter because of the input beam. Unlike the linear propagation of light where the spectral and spatial components of light do not affect each other in a medium, the nonlinear interaction of light with matter gives rise to complex coupling between the light components through the medium [2]. These effects have been very often regarded as detrimental to fiber-based optical communication systems [3]. However, they also offer new and exciting potential applications, such as devices in which light can be controlled by light [4]. Due to their strong light confinement capabilities, optical fibers have been early recognized as an ideal medium to exploit the nonlinear effects for all-optical processing applications in telecommunication and fiber laser industries [5]. This research field has recently been dramatically stimulated by the development of a new generation of highly nonlinear optical fibers which has an array of tiny holes running through the whole length of the fiber. These so-called photonic crystal or microstructured fibers allow conversion of a single colour laser beam into a white light supercontinuum spanning two octaves in frequency [6] (i.e., a laser rainbow extending from the ultra-violet well into the infra-red as shown in Figure 3.1). This new light source has revolutionized optical metrology, making absolute measurements of optical frequencies with unprecedented accuracy, and optical coherence tomography (OCT) with enhanced resolution.
This course is intended to provide an overview of nonlinear fiber optics in a way that is simultaneously accessible and technically comprehensive. First, we will describe some basic concepts of nonlinear propagation in dielectrics, so as to understand the origin of the main third-order nonlinear effects in fused silica, namely the optical Kerr effect and the stimulated Raman scattering (SRS). The former, which arises from the distortion of electronic structure of silica molecules, gives rise to an instantaneous intensity-dependent refractive index. We will see that the Kerr effect leads to several intriguing phenomena such as self- and cross-phase modulation, optical solitons, modulation instability, four-wave mixing, and parametric amplification. Then we will describe stimulated Raman scattering (SRS) that results from vibrational states of silica molecules and allows efficient down-frequency conversion.

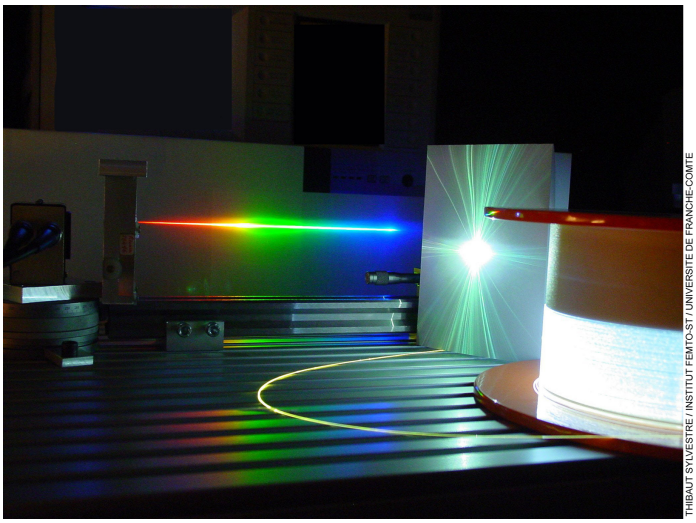

Fig. 1. This image shows white-light supercontinuum generation by injecting an intense 800-nm femtosecond (10^{-15} s) laser beam into a 50-m long photonic crystal fiber.

1. Nonlinear propagation in fused silica

1.1 Nonlinear propagation in dielectrics: basic concepts

The glass composing fibers is considered as an isotropic and homogeneous dielectric medium exhibiting the linear and dispersive behaviours. The response of fibers is quantified by the polarization density induced in the medium $P(t)$. This polarization density presents a non-instantaneous response to an external excitation, which in fact is responsible for the dispersive effects in the fiber. The polarization response of the medium $P(t)$ at a given time t is the superposition of the effects of $E(t')$ at any previous time $t' \leq t$ [4]. This means that, mathematically, the response of the medium can be represented as the convolution of a response function by an external stimulation (as in any other linear system). In the case of a dispersive dielectric material, the response function is given by a time-dependent electric susceptibility and the total response of the medium is given by the convolution of the electric susceptibility with the applied electric field:

$$P(t) = \varepsilon_0 \int_{-\infty}^{+\infty} \chi(t') E(t-t') dt' = P_L \tag{1}$$

Compared to the "conventional" (linear) propagation, the main difference of nonlinear propagation of light is the additional terms which are introduced in the polarization density to explain properly its behavior. Although $P(t)$ requires in general a quantum-mechanical description, it has been proved that, if the optical carrier frequency is far away from medium resonances, it can be expressed as function of the applied electric field E by the relation [2]:

$$\begin{aligned} P(t) &= P_L + P_{NL} = \varepsilon_0 \int_{-\infty}^{+\infty} \chi^{(1)}(t') E(t-t') dt' + \\ &+ \varepsilon_0 \int_{-\infty}^{+\infty} \int_{-\infty}^{+\infty} \chi^{(2)}(t',t'') : E(t-t') E(t-t'') dt' dt'' + \\ &+ \varepsilon_0 \int_{-\infty}^{+\infty} \int_{-\infty}^{+\infty} \int_{-\infty}^{+\infty} \chi^{(3)}(t',t'',t''') \vdots E(t-t') E(t-t'') E(t-t''') dt' dt'' dt''' + \ldots \end{aligned} \tag{2}$$

Note that each element $\chi^{(i)}$ is a tensor of rank i. Therefore the products inside the integrals are tensor products. Since fiber is an isotropic medium, the tensor $\chi^{(1)}$ can be described by a single non-zero element and the tensor $\chi^{(3)}$ has only four non-zero elements, which are related to Kleinman symmetry rules [7].

This description can also be adopted in a dispersive medium when the electric-dipole approximation is valid. In this approximation, the electromagnetic wavelength involved in the transition between different atomic energy levels is much larger than the typical size of the atoms or molecules taking part in the transition. Such conditions are largely satisfied in nonlinear fiber optics, so we will consider hereafter that the electric-dipole approximation is valid.

In addition, silica molecules present inversion symmetry (the molecule is said to be centrosymmetric). This means that the properties of the material can not alter by the transformation $r \rightarrow -r$, i.e. the polarization vector is reversed when the electric field is reversed: $P(-E) = -P(E)$. In this case, the relation between P and E must exhibit odd symmetry, so that all the even terms in the expansion vanish. Thus, only the odd terms in the expansion are retained (typically, only up to the third-order).

Different processes take place depending if medium presents a second-order or a third-order nonlinearity. In particular, second-order nonlinear effects (due to $\chi^{(2)}$) occur only in non-centrosymmetric crystals, because they do not present inversion symmetry. In this case, the dominant non-linear processes are: second-harmonic generation, sum- and difference-frequency generation and optical parametric oscillation. Third-order non-linear interactions (due to $\chi^{(3)}$) can occur in any material. They lead, among others, to the following processes: third-harmonic generation (THG), intensity-dependent refractive index (Kerr effect, including self-phase modulation (SPM) and self-

focusing), four-wave mixing (FWM), stimulated Brillouin scattering (SBS) and stimulated Raman scattering (SRS).

The effects occurring in a third-order nonlinear medium can be related to the different physical processes that result in the nonlinear response [2]. A summary of the physical mechanisms that contribute to the nonlinear susceptibility of fused silica can be found in Table 3.1. There are three important contributions responsible for the third-order susceptibility: (1) the instantaneous polarisation contribution caused by the response of bound electrons to the applied electric field (responsible for the Kerr effect); (2) the molecular re-orientation contribution slightly delayed (responsible for the Raman effect) and (3) the electrostriction contribution in the fiber (responsible for the Stimulated Brillouin Scattering). The first two effects will be addressed in this course. Stimulated Brillouin Scattering, which is very efficient in optical fibers, will be briefly described.

Table 1. Optical effects that contribute to the third-order susceptibility of fused silica.

Physical mechanism	Chi3 [esu]	Response time [sec]	Related optical process
Electronic polarization	$1.8 \cdot 10^{-14}$	< 1 fs	Kerr effect and related phenomena
Molecular re-orientation	$3.2 \cdot 10^{-15}$	$100 \cdot 10^{-15}$	Stimulated Raman Scattering (SRS)
Electrostriction (acoustic)	$2 \cdot 10^{-12}$	$10 \cdot 10^{-9}$	Stimulated Brillouin Scattering (SBS)

1.2 Optical Kerr effect

In order to understand the effects occurring in fused silica, it is customary to study separately the three contributions from the nonlinear susceptibility. To understand the implications of nonlinear propagation, we will consider the Kerr effect isolated (which is relatively simple to treat mathematically). As mentioned before, this effect is caused by the nonlinear response of bound electrons and can be considered as an instantaneous effect to the nonlinear susceptibility. Therefore the elements of the third order susceptibility tensor can be written as $\chi_{ijkl}^{(3)}(t,t',t'') = \chi_{ijkl}^{(3)} \cdot \delta(t) \cdot \delta(t') \cdot \delta(t'')$, and the nonlinear contribution to the polarization induced in the medium would read:

$$P_{NL}(t) = \varepsilon_0 \chi^{(3)} \vdots E(t)E(t)E(t) \tag{3}$$

This shows clearly that the polarization density in the medium is sensitive to the third-order power of the field amplitude. We can now inject a linearly-polarized monochromatic wave $E(t)=E_0\cos(\omega t)$ into a nonlinear medium described by equation (2). The polarization density reads:

$$P(t) = \varepsilon_0 \left(\chi^{(1)} + \frac{3\chi_{xxxx}^{(3)}}{4} \left| E_0 \right|^2 \right) E_0 \cos(\omega t) + \varepsilon_0 \frac{\chi_{xxxx}^{(3)}}{4} E_0^{\,3} \cos(3\omega t) \tag{4}$$

The terms with the frequencies ω and 3ω appear in the equation. The term with 3ω is responsible for the third-harmonic generation (THG). The terms with ω are responsible for self-phase modulation. To see this more clearly, we can write the response of the medium at the frequency ω as a first-order response:

$$P(t) = \varepsilon_0 \chi E_0 \cos(\omega t) \qquad \text{where} \qquad \chi = \chi^{(1)} + \frac{3\chi_{xxxx}^{(3)}}{4} \left| E_0 \right|^2 \tag{5}$$

In fact, the effective refractive index of the fiber results from the above relationship where the light intensity impacts on the refractive index, as shown in the equation:

$$n_{eff} = \sqrt{1+\chi} \cong n_0 + \frac{3\chi^{(3)}}{8n_0} \left| E_0 \right|^2 = n_0 + n_2 I \tag{6}$$

where a Taylor series expansion is performed. It is assumed that the nonlinear (intensity-dependent) part of the refractive index is very small compared to the constant part. The coefficient n_2 is called the Kerr coefficient, and its value is around $3.2 \cdot 10^{-20}$ m^2/W for fused silica. The value of n_2 is dependent

only on the medium. However it may vary from one fiber to another. This is mainly due to the fact that silica fibers are doped with GeO_2. Higher the GeO_2 doping is, larger the value of n_2 is obtained.

The main consequences of this third-order nonlinear response are the following:

- The refractive index of medium depends on light intensity. As a result, the phase velocity of an optical field in a nonlinear medium depends on its own intensity.
- The carrier frequency of an optical field with varying intensity will alter when it travels through a nonlinear medium (phase changes with time imply frequency changes).
- The principle of superposition is violated. Different optical fields propagating in a single nonlinear medium will interact among them and create new frequencies.
- Light can interact with light: an intense optical field can modify the refractive index of medium which, in its turn, can modify the phase of another optical wave. Nonlinear optics allows, therefore, an all-optical control of light.

2. Nonlinear propagation in optical fibers

Single-mode optical fibers are highly-confined optical media in which the light travels through a very small cross-section, and normally over a very long propagation distance. The structure and properties of the guide (mode area, absorption, dispersion, etc) have a direct impact on its nonlinear properties[4]. This section reviews some important definitions that we will use for the rest of the lecture. We will also provide an introduction to the basic equation governing nonlinear propagation in optical fibers: the Nonlinear Schrödinger equation (NLSE).

2.1 Important definitions

As we saw in the previous section, nonlinear effects depend on light intensity. It is important to note this fact since it has a direct impact on all the relevant parameters of our study. The intensity of an optical field is the optical power transmitted per unit area (measured in W/m^2). Qualitatively speaking this means that, for a given input power, the nonlinear effects will be higher when the cross section of the guided mode is smaller. Since the size and shape of the guided mode is a function of the refractive index profile, we need some parameters to evaluate the efficiency of the nonlinear effects in the fiber. The most important parameter for this evaluation is the *effective area*[4]. The effective area measures the area that is effectively occupied by the mode to generate the nonlinearities and it is related to the normalized mode field distribution $F(x,y)$ through the relationship :

$$A_{eff} = \frac{\left(\int\int_{-\infty}^{+\infty} |F(x,y)|^2 \, dxdy \right)^2}{\int\int_{-\infty}^{+\infty} |F(x,y)|^4 \, dxdy} \tag{7}$$

Typical values of effective area at 1550 nm are 80 μm^2 for conventional single-mode (SMF) fibers (with the zero-dispersion at 1300 nm), and 50 μm^2 for dispersion-shifted (DSF) fibers. It is thus clearly expected that nonlinear effects are generally 1.6 times more efficient in DSFs than in SMFs. In terms of applications, there is a more interesting parameter to measure the efficiency of the nonlinear effects which is called the *nonlinear coefficient* :

$$\gamma = \frac{kn_2}{A_{eff}} = \frac{\omega_0 n_2}{cA_{eff}} \tag{8}$$

where k is the wave vector and ω_0 is the center frequency of the wave injected into the fiber. This coefficient measures the phase shift (in radians) per unity power and unity length, which is self-induced by an optical wave propagating in the fiber. Typical values are 1.3 $W^{-1} \cdot km^{-1}$ for conventional SMFs and around 2 $W^{-1} \cdot km^{-1}$ for DSFs.

Finally, it is important to note that fibers are particularly long nonlinear optical media (tens of kilometers). In most transparent nonlinear media, losses (pump absorption, scattering, etc) can be neglected since the interaction distances are short and the losses are very low. In optical fibers, however, even though the losses are the lowest of any known optical material, the very long

interaction distances lead to a significant power loss of an intense beam during the propagation. In result, the phase shifts per kilometer will be higher in the beginning part of the fiber than in the end part. Therefore it is important to define the *effective length*:

$$L_{eff} = \int_0^L e^{-\alpha z} dz = \frac{1 - e^{-\alpha L}}{\alpha} \tag{9}$$

The effective length measures the length with which a lossless fiberfiber would exhibit the same nonlinear effect as in a real lossy fiberfiber.. When α=0, L_{eff}=L and when α>0, L_{eff}<L. Thus L_{eff} becomes smaller as the loss increases. Note that as L increases, the effective length converges to the value $1/\alpha$ (as $L\to\infty$, $L_{eff}\to 1/\alpha$). The value $1/\alpha$ for standard SMFs is approximately 22 km at 1550 nm.

2.2 The Nonlinear Schrödinger Equation (NLSE)

The Nonlinear Schrödinger Equation is the basic equation describing the propagation of an intense optical beam in a fiber. We can understand the origin of the equation by rewriting the paraxial propagation equation (in the frequency domain) of the complex field $\tilde{E}$:

$$\frac{\partial^2 \tilde{E}}{\partial z^2} + \left(n_{eff} k_0\right)^2 \tilde{E} + k_0^2 \tilde{P}_{NL}(\omega) = 0 \tag{10}$$

where n_{eff} is the effective index of fiber, assuming linear propagation and $\tilde{P}_{NL} = P_{NL}(\omega) e^{j\beta_0 z}$ is the nonlinear component of polarization in the frequency domain (which propagates with the electric field). Unlike the linear case, the propagation is perturbed by the term taking into account the nonlinear contribution due to Kerr effect (which is assumed small all over this derivation). To understand the effects in the time domain, we can insert a solution of the type:

$$\tilde{E}(z, \omega - \omega_0) = A(z, \omega - \omega_0) e^{j\beta_0 z} \tag{11}$$

We can thus obtain the next equation:

$$\frac{\partial^2 A}{\partial z^2} + 2j\beta_0 \frac{\partial A}{\partial z} - \beta_0^2 A + \left(n_{eff} k_0\right)^2 A + k_0^2 P_{NL} = 0 \tag{12}$$

To obtain a meaningful result, we now have to invoke the slowly-varying envelope approximation (SVEA). In this approximation, it is assumed that the complex amplitude $A(z,t)$ varies slowly only with z and t. Therefore, the second order derivatives can be neglected, obtaining:

$$\frac{\partial A}{\partial z} - j(n_{eff} k_0 - \beta_0) A - j \frac{k_0^2}{2\beta_0} P_{NL} = 0 \tag{12}$$

where we assume that $n_{eff}k_0+\beta_0 \cong 2\beta_0$. We can now expand $n_{eff}k_0$ by means of a Taylor series expansion around ω_0 to take into account dispersion effects:

$$n_{eff} k_0 = \beta_0 + \beta_1(\omega - \omega_0) + \frac{\beta_2}{2}(\omega - \omega_0)^2 + \ldots \tag{13}$$

Inserting this expansion into equation (12) and recalling the properties of the Fourier transform of a derivative, we can finally write the NLSE in the time domain:

$$\frac{\partial A}{\partial z} + \beta_1 \frac{\partial A}{\partial t} + i \frac{\beta_2}{2} \frac{\partial^2 A}{\partial t^2} = i\gamma |A|^2 A \tag{14}$$

where the amplitude units are assumed normalized so that the instantaneous power is $P=|A|^2$. For convenience, it is customary to re-write this equation in terms of a moving frame around the signal $\tau=t-\beta_1 z$:

$$\frac{\partial A}{\partial z}+i\frac{\beta_2}{2}\frac{\partial^2 A}{\partial \tau^2}=i\gamma|A|^2 A \tag{14}$$

This equation can be generalized to include losses, Raman Scattering, self-steepening and shock-wave formation deriving the Generalized Nonlinear Schroedinger Equation (GNLSE) [8]:

$$\frac{\partial A}{\partial z}=i\sum_{m\geq 2}^{m=12}\frac{i^m\beta_m}{m!}\frac{\partial^m A}{\partial \tau^m}+i\gamma\left[1+\frac{i}{\omega_0}\frac{\partial}{\partial \tau}\right]\times\left[A(z,\tau)\int_{-\infty}^{+\infty}R(\tau')\left|A(z,\tau-\tau')\right|^2 d\tau'\right]-\frac{\alpha(\omega)}{2}A \tag{15}$$

Dispersion effects are described by the first term on the right hand side of Eq. (13) (up to 12th order) while nonlinear optical effects such as Self-Phase Modulation, SRS, self-steepening and shock-wave formation are described by the second one. $R(\tau)=(1-f_R)\delta(\tau)+f_R\cdot h_R(\tau)$ is the nonlinear response of silica, including instantaneous (first term, Kerr) and delayed (second term, Raman) effect. $f_R=0.18$ is the Raman contribution to the Kerr effect and $h_R(\tau)$ is a function describing the delayed Raman response in the time domain in silica.
It must be stressed in this derivation that the polarization of the optical wave is assumed linear and constant along the fiber. Although this is not the real case, it is shown empirically that equation (15) gives a good approximation of the phenomena occurring in the optical fiber. To take into account the polarization evolution along the fiber, two coupled NLSEs (one for each polarization axis) have to be integrated.

3. Self- and Cross-phase modulation

3.1 Self-Phase Modulation (SPM)

Self-phase modulation is one of the first manifestations of the optical Kerr effect. It was first observed in liquids in 1967 [9] and later in other optical media such as optical fibers [10]. Self-phase modulation is in fact the self-induced phase and frequency changes that occur in an intense optical pulse which travels through an optical fiber. The intensity-dependent refractive index results in the pulse to modulate its own optical phase according to its intensity profile. Such effect is qualitatively shown in figure 3.2. Consider an electric field E_1 propagating through an optical fiber. Because of the Kerr effect, the pulse will create a refractive index variation, being the greatest at the maximum of the pulse intensity profile. This means that a nonlinear phase shift Φ_{NL} varies across the pulse. Therefore, compared to the tails, the peak of the pulse suffers from a larger nonlinear phase shift. This varying phase shift across the pulse can also be seen as a frequency chirp (the instantaneous frequency is the derivative of the phase with respect to time) that leads to spectral broadening. Thus red-shifted (Stokes) and blue-shifted (anti-Stokes) frequencies symmetrically appear in the leading and the trailing edges of the optical pulse, respectively. The beating of these new frequencies will produce some interference fringes in the pulse spectrum. The number of fringes N is proportional to the nonlinear phase shift by $N\pi$. This behavior is illustrated in Figure 3.3 that shows the SPM-induced spectral broadening of a high-peak power picosecond pulse propagating in a short SMF.

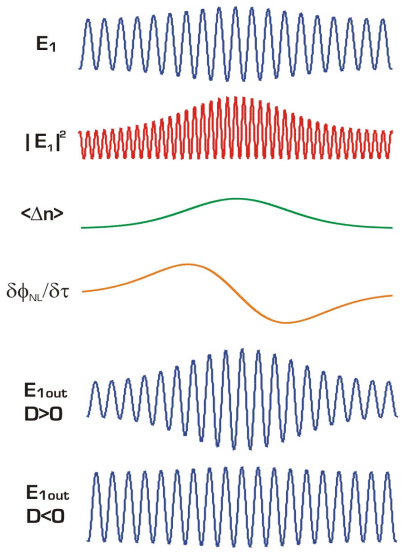

Figure 2 : Qualitative illustration of the effects of self-phase modulation and modulation instability.

We can easily quantify this spectral broadening using equation (14) (lossless NLSE) if we assume no dispersion in the fiber (β_2=0). The output amplitude reads as:

$$A(z,t) = A(0,\tau)\exp\left(j\gamma L|A|^2\right) \tag{16}$$

The instantaneous frequency change imposed on a Gaussian pulse $|A(\tau)|^2 = P_0 \exp\left(-\tau^2/\tau_0^2\right)$ would be:

$$\delta\omega(t) = -\gamma L \frac{\partial}{\partial t}|A|^2 = 2\gamma P_0 L \tau \exp\left(-\frac{\tau^2}{\tau_0^2}\right) \tag{16}$$

By taking into account optical loss in the fiber, L should be replaced by L_{eff}. As we can see in figure 3.2, there is a linear frequency variation at the centre of a Gaussian pulse. This variation (called chirp in the linear case) is positive $C=2\gamma P_0 L$. When a positively chirped pulse is introduced in a fiber with negative β_2, one can obtain a compression of the pulse width. This is the basis of SPM-based pulse compressors.

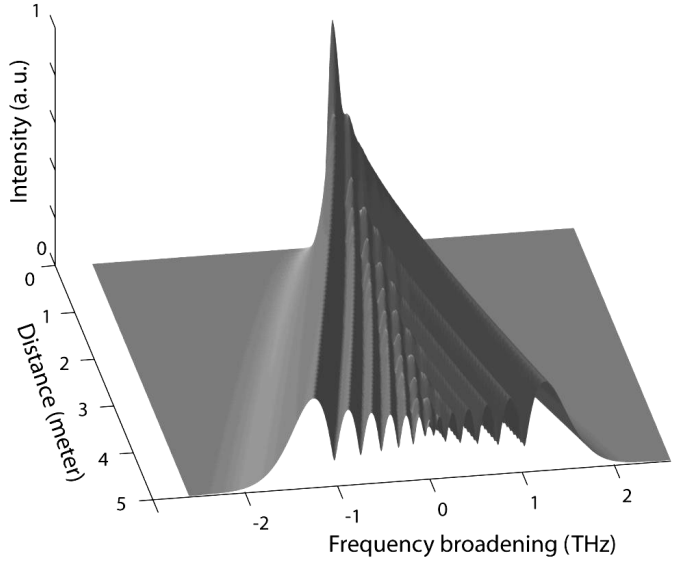

Figure 3 : Self-phase modulation-induced spectral broadening of a picosecond pulse propagating in a short single-mode optical fiber. The figure is obtained from a numerical simulations of Eq. (14) with the following parameters: L=5m, γ=50W^{-1}km^{-1}, P=12 W, τ_0=30ps, and β_2=0.

Cross-phase modulation (XPM) results from the phase changes of an optical wave induced by a second optical wave with different wavelength or polarization, or propagating in different modes of a multimode fiber. In this case, the nonlinear phase shift depends on the polarization states of the two interacting waves. The shiftis two thirds smaller than SPM for an orthogonal polarization and twice larger than SPM for the same linear polarization and different wavelengths (or modes). The orthogonal polarization case, which is called degenerate XPM, occurs in birefringent optical fiber. It is schematically sketched in Figure 3.4 with an incoming pulse polarized at 45° of the fiber birefringent axes. The input pulse will split into a fast and a slow component. Therefore, XPM leads to pulse frequency chirp and group-velocity mismatch between the fast and slow components propagating in a birefringent fiber.

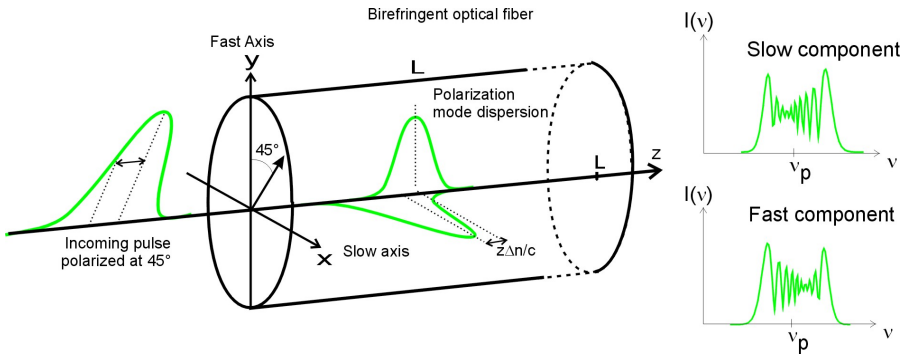

Figure 4 : Principle of degenerate cross-phase modulation in a birefringent optical fiber.

3.2 An application of SPM and XPM: The Nonlinear Optical Loop Mirror (NOLM)

A very interesting device that can advantageously exploit the effects of SPM and XPM is the Nonlinear Optical Loop Mirror (NOLM) [5][11]. In its simplest configuration, the NOLM is based on a Sagnac fiber loop in which an attenuator is placed at the end of a loop. Thus the attenuator introduces a power imbalance between the clock-wise and counter-clockwise propagating fields in the loop. In linear operation, the Sagnac mirror acts as a perfect mirror. The input pulse is split by a directional coupler into two counter-propagating electric fields, as shown in Figure 3.5. After a propagation through the loop the two fields are re-combined at the coupler. Since they travel through the same path with the opposite direction, the optical path length is identical to both the counter-propagating fields, producing the same linear phase shifts. As a result, the input pulse is totally reflected into the input port. Therefore, for low input powers the loop acts as a perfect mirror, and no light exits to the output port. A polarization controller is used in the loop to optimize the interference and ensure a total reflection of the light at low powers. In the high power regime, however, the refractive index of the fiber is modified by the light intensity. This means that the imbalance of the optical powers in the two arms caused by the attenuator leads to a difference of the effective optical path lengths for the clockwise and counter-clockwise pulses.

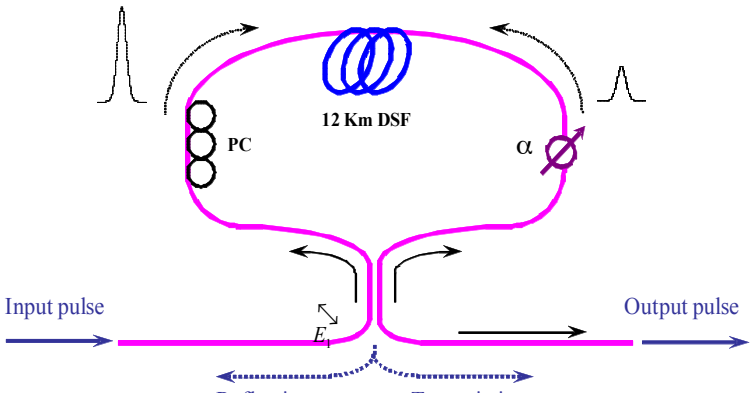

Figure 5 : The Nonlinear Optical Loop Mirror as pulse compressor.

The transmission coefficient T of this device can be written as a function of the phase difference between the two arms:

$$T = \alpha \sin^2\left(\frac{\Delta\varphi_{NL}}{2}\right) \tag{16}$$

where

$$\Delta\varphi_{NL} = \frac{\gamma P_0 L}{2}(1-\alpha) \tag{17}$$

P_0 being the input power. Thus, the system behaves like a saturable absorber: the transmission grows for higher input powers, with a quadratic dependence on the power for small accumulated nonlinear phase shifts. Since the power in the peak of the pulse is larger than in the wings, the output pulse is sharper than that at the input, resulting in pulse compression[12]. One negative aspect of the NOLM is that the phase of the output pulse is also altered by SPM. Therefore, the device induces a chirp in the signal. The chirp can be reduced by adding an anomalously dispersive fiber onto the output of the NOLM.

Some more interesting features arise when two beams are combined in the Sagnac loop. In this case, one can use the effect of XPM to provide the nonlinear phase shifts required to imbalance the interferometer. With this configuration, some interesting all-optical functions can be achieved such as wavelength conversion, ultra-high speed de-multiplexing [13], rapid all-optical switching [14].

4. Optical Solitons

A fundamental optical soliton is a wave-packet or pulse that preserves its shape during the propagation, being unaffected by dispersion and nonlinearities [16]. Qualitatively speaking, fundamental solitons can simply be understood as an equilibrium between pulse sharpening that occurs in the anomalous dispersion regime through SPM and pulse spread that occurs due to anomalous dispersion in a fiber [16]. A soliton is obtained just by the adequate balance between Kerr effect and dispersion, which enables essentially no distortion on the pulse (in other words, the distortions mutually compensate).

Scalar solitons appear only when the fiber exhibits anomalous dispersion. In this case, fundamental solitons are the only stationary solutions of the NLSE. This is, solitons are the unique transmission format that allows transmission without distortion. The existence of soliton solutions of the NLSE can be easily verified by inserting the following solution into the NLSE:

$$A(z,t) = \sqrt{P_0}\,\mathrm{sec}\,h\left(\frac{\tau}{\sqrt{\beta_2/\gamma P_0}}\right)\exp\left(i\frac{\gamma P_0}{2}z\right) \tag{20}$$

Thus, fundamental solitons have the shape of a hyperbolic secant. Fundamental solitons are obtained only when the following condition is satisfied:

$$N = \sqrt{\frac{\gamma P_0 T_0^2}{|\beta_2|}} = 1 \tag{21}$$

where T_0 stands for the temporal width of the pulse. It is expected from the equation that a strict balance is required between peak power, duration of the soliton and dispersion in fiber to achieve such un-distorted transmission. It must be mentioned that breathing or periodic solutions can be obtained for integer $N>1$. These solutions are known as higher-order solitons. For instance, Figure 3.6 shows a third–order periodic soliton propagating in a 2-km single-mode optical fiber. In particular it is clearly seen that the dynamic solutions show pulse collapse, splitting and then soliton recovery in the fiber. These solutions are however unstable because of higher-order dispersion and Raman effects. For this reason, they tend to split into several fundamental solitons during the propagation and to shed energy in the form of frequency-shifted dispersive waves [17]. This is the basis of supercontinuum generation [18].

Solitons were first demonstrated in 1980 in an experiment in Bell Labs [19]. Since then, they have been widely demonstrated for a robust transmission format in many areas. In an experiment in 1989,

solitons were propagated without significant degradation over more than 10,000 km with periodic amplification [20]. One of the interesting properties of solitons is that they tend to adapt their parameters through the propagation so as to satisfy the soliton condition given by equation (20). If one of the parameters is modified (for instance, the dispersion of the fiber), the soliton will adapt the rest of the parameters to keep N=1. This is the basis of adiabatic soliton compression in dispersion decreasing fibers [21]: as the fiber dispersion decreases along the fiber, the soliton width T_0 decreases as well to keep N=1.

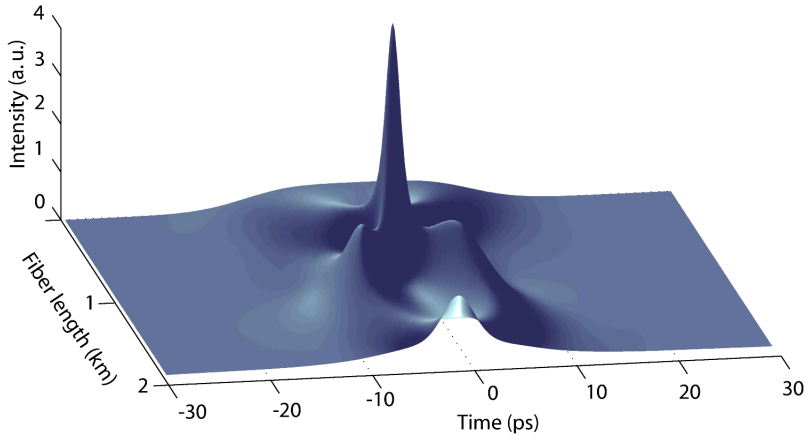

Figure 6. Third-order soliton (N=3) propagating in a 2 km-long single-mode fiber obtained from a numerical simulation of Eq. (14) with the following parameters : L=2 km, γ=2 $W^{-1}km^{-1}$, P=250 mW, τ_0=10ps and β_2=–9 ps^2/km.

5. Modulation instability (MI)

As in the case of solitons, modulation instability (MI) is a non-linear phenomenon that has been observed in several branches of physics such as plasma physics, hydrodynamics, or matter waves [22]. In optics, it occurs when the steady-state of an electromagnetic field becomes unstable due to an interplay between anomalous dispersion and nonlinearity in a medium. MI is initiated by SPM and manifests as the break-up of a continuous field into a train of ultra-short pulses. As the typical MI oscillation frequency ν_{MI} is of the order of 0.1 to 1 THz, pulses with temporal duration $\tau >> 1/\nu_{MI}$ can be considered quasi-cw respect to this instability, that is, pulses usually longer than 10 ps. In the frequency domain, it gives rise to two sidebands (Stokes and anti-Stokes) around the center frequency of a quasi-monochromatic cw field. Together with four-wave mixing, this process leads to the generation of many equally-spaced frequency components. These latter ones interfere each other in a similar way to that in a mode-locked laser and produces a pulse train. Modulation instability plays a fundamental role in supercontinuum generation with cw pumping.

Modulation instability can also be qualitatively understood from Figure 3.2. We consider a quasi-cw electric field E_1 propagating through an optical fiber. This field induces a small intensity perturbation. Because of Kerr effect, this intensity perturbation will create a refractive index variation, being the largest at the point of maximum intensity of the field. Therefore, a varying nonlinear phase shift Φ_{NL} affects the signal and the peak of the perturbation suffers from a nonlinear phase shift larger than that in the valleys. As in the previous case, this varying phase shift across the pulse can also be considered as a frequency chirp. The leading edge of the perturbation is shifted towards the blue and the trailing edge towards the red. Now the key point is to consider what happens in the different dispersion regimes. When the dispersion is normal (β_2>0, D<0), the red shifted components travel more slowly than the blue ones. In result the trailing edge lags compared to the leading edge and the intensity perturbation profile spreads out. On the other hand, when the dispersion is anomalous (β_2<0, D>0), the trailing edge travels faster than the leading edge, thus it allows sharpening of the intensity perturbation profile. As the profile becomes sharper, the whole process can be reinforced, thus leading to an exponential amplification of the perturbation.

The process can be described mathematically by a stability analysis of a CW solution of the NLSE. That results in creating gain bands at both side of the pump frequency, the gain coefficient being :

$$g(\Omega) = |\beta_2 \Omega| \sqrt{\frac{4\gamma P_0}{|\beta_2|} - \Omega^2} \tag{18}$$

where $\Omega = \omega - \omega_0$ is the frequency detuning between the pump and the frequency component analyzed. A simple analysis of this gain curve reveals two maxima at a detuned frequency:

$$\Omega_{max} = \pm \sqrt{\frac{2\gamma P_0}{|\beta_2|}} \tag{19}$$

This frequency can be interpreted as follows: as we have briefly described at the beginning of this section, the effect of MI causes a spontaneous break-up of an intense cw light into a pulse train. The most amplified spectral components are those oscillating at frequency Ω_{max}. This leads to two symmetric sidebands at frequency $\omega_0 \pm \Omega_{max}$ (anti-Stokes and Stokes) in the frequency domain. In the time domain, it generates a pulse train with period $T_M = 2\pi/\Omega_{max}$. Ω_{max} is thus the repetition rate of the generated pulse train, as shown in Figure 3.7. MI can also be stimulated with an optical seed at the fiber input whose frequency matches the modulation frequency. In this case, it refers to induced MI whereas in the absence it is spontaneous MI. We will see in section 3.7 how induced MI involves in optical parametric amplification.

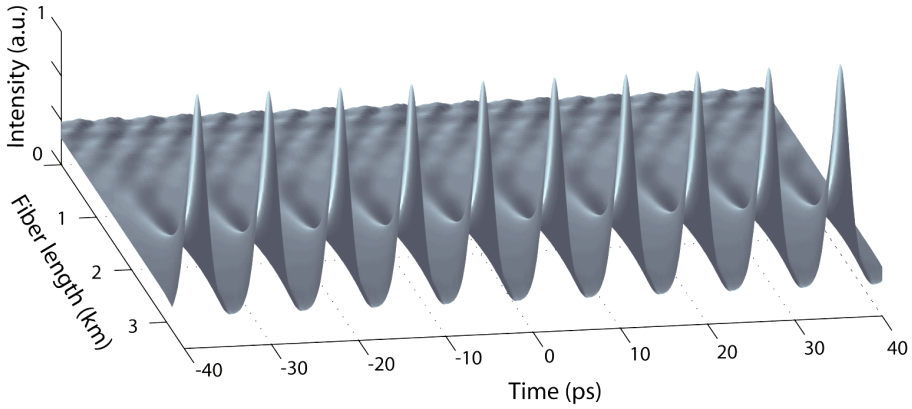

Figure 7 : Modulation instability of a noisy continuous field and a soliton-like pulse train generated in a single-mode optical fiber, obtained from a numerical simulation of Eq. (14) with the following parameters: L=3km, γ=2W^{-1}km^{-1}, P=500 mW and β_2=–9 ps^2/km.

6. Four-wave mixing (FWM)

6.1 Origin of four-wave mixing

Third-order nonlinearities allow generation of new frequency components when two or more waves with different frequencies exist in a fiber [24]. This effect is generally known as four-wave mixing (FWM) phenomena. In order to understand the origin of new frequencies, the interested reader is invited to insert two fields at different frequencies (ω_1 and ω_2) in the expression of the polarization density (equation (3)) and check the frequencies of the resulting terms. In addition to third-harmonic, self-phase and cross-phase modulation terms, new terms at frequencies $2\omega_1 \pm \omega_2$ and $2\omega_2 \pm \omega_1$ appear. Conventionally, frequencies ω_1 and ω_2 are close, so the terms with $2\omega_1 - \omega_2$ and $2\omega_2 - \omega_1$ will fall close to the frequencies of two input waves whilst the terms with other frequencies will fall very far from those of the two waves. It is expected from phase matching conditions (see below) that the terms with far frequencies tend to vanish, while the terms with close frequencies (which satisfy phase matching relations) grow over the fiber distance.

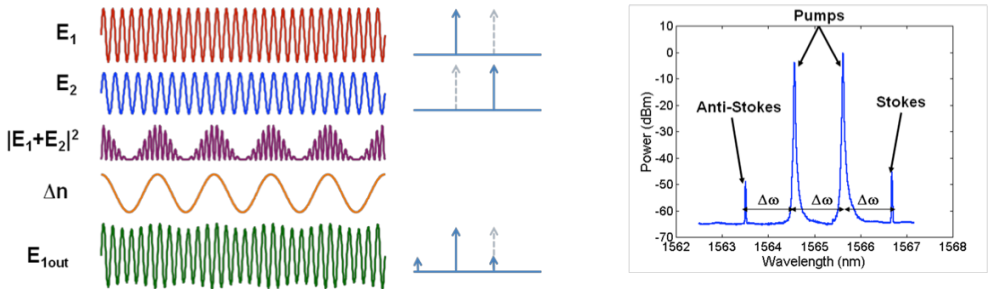

Figure 8: Left: Qualitative explanation of the effect of four-wave mixing. Right: Spectrum of a simple FWM experiment performed in a dispersion-shifted fiber.

A qualitative explanation of the effect of FWM can be seen in figure 3.8. Two beams E_1 and E_2 combine in the optical fiber. The interference between the two creates a beating intensity pattern at a frequency of $\omega_1-\omega_2$. This intensity pattern will induce a refractive index grating in the fiber, which will, in turn, introduce a small phase modulation on both fields E_1 and E_2. Practically, a small phase modulation on E_1 will give rise to two sidebands at both sides of ω_1, thus creating small contributions to ω_2 and $2\omega_1-\omega_2$. The similar process will apply to E_2, hence creating contributions to ω_1 and $2\omega_2-\omega_1$.

6.2 Phase-matching

The above description holds well for short fibers. In order to consider the effect in long fibers, one should consider the sum of all the FWM contributions generated in many short fibers. The main intuitive conclusion is that the growth of the mixing product along the fiber will depend whether the contributions from all the short fibers add in phase or not. For optimum conversion efficiency, all the contributions from all the short fibers needs to be added in phase. This leads to the condition that the phase mismatch between the generated FWM contribution and the propagating wave at the FWM frequency should be zero. If we consider the FWM product at $\omega_s=2\omega_1-\omega_2$, the phase mismatch will be:

$$\Delta\beta = 2\beta(\omega_1)-\beta(\omega_2)-\beta(\omega_s) \tag{21}$$

called the phase matching condition. *Phase matching conditions* appear in many nonlis appear in many nonlinear optical processes. The nonlinear processes that depend on phase matching condition are called phase-sensitive processes. Examples of other phase-sensitive processes are frequency doubling, sum and difference frequency generation, and parametric amplification and oscillation.

We can get some more insight on the implications of this phase matching condition by using the Taylor series expansion of the propagation constant Eq. (13) around ω_1. The result is:

$$\Delta\beta = \beta_2(\omega_2-\omega_1)^2 + \frac{\beta_4}{12}(\omega_2-\omega_1)^4 + \ldots \tag{22}$$

Considering the small value of the fourth-order term, the only possibility to satisfy phase-matching condition is to work in the zero-dispersion wavelength region of the fiber ($\beta_2=0$) [25].

7 Optical Parametric Amplification (OPA)

7.1 Principle of parametric amplification

The underlying nonlinear process for parametric amplification is the optical Kerr effect which causes a refractive index variation proportional to the local intensity of light [26][27][28]. When a high-power pump wave and a frequency-detuned small signal wave travel together in an optical fiber, they produce interference beats and modulate the refractive index via the Kerr effect, leading to the generation of a light-induced moving index grating. This phenomenological approach is schematically sketched in Figure 3.9. In such a scheme, parametric amplification can be seen in the time domain as an energy transfer from the pump to both the signal and idler waves by a diffraction-like process on the refractive index grating. In the frequency domain, parametric amplification can be viewed as a four-wave mixing (FWM) process, as previously described in section 3.6, where the pump and the signal are both present at the fiber's input. When phase matching is fulfilled, exponential-like amplification of the signal together with generation of an idler wave is possible. The phase matching condition and the parametric gain are linked to the index grating period and the grating contrast, respectively. From a physical point of view, OPA is formally equivalent to the induced MI process described in section 3.5 since the incoming continuous pump wave breaks up into high-contrast amplitude modulations in the form of ultra-short optical pulses, as shown in Figures 3.7 and 3.9. MI is studied in the time domain whereas OPA is commonly investigated in the Fourier domain. Both terms are now recognized and used in the literature. However, MI and OPA do not manifest themselves in exactly the same situations. OPA occurs for moderate values of the nonlinear phase shift γPL whereas spontaneous MI requires higher values of γPL to be clearly observed.

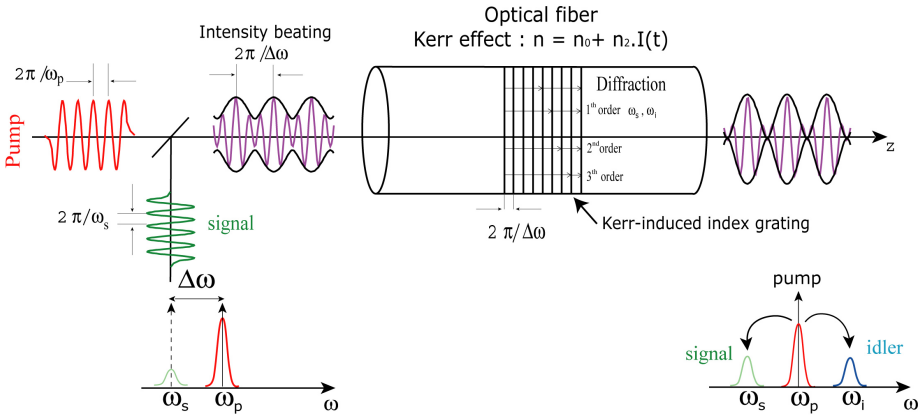

Figure 9 Principle of parametric amplification in optical fiber through the optical Kerr effect.

When there is no input signal, OPA can be considered as the effect of amplifying vacuum or quantum noise. The resulting parametric amplified spontaneous emission (ASE) is considered as a detrimental noise source for optical amplification. It can however be reduced when fiber OPA functions in a phase-sensitive configuration, i.e., when the three waves including the idler propagate in a controlled relative phase [26].

7.2 Parametric gain and bandwidth

As mentioned in section 3.6, phase-matching in the third telecommunication band at 1.55 µm is generally achieved near the zero-dispersion wavelength of dispersion-shifted fibers (DSF) to provide broadband operation and high gain at telecommunication wavelengths. The parametric gain of the signal is then given by the following expression [26]:

$$G = 1 + \left(\frac{\gamma P}{g} \sinh\left(g L_{eff} \right) \right)^2 \tag{23}$$

where $g^2 = (\gamma P)^2 - (\kappa/2)^2$ is the parametric gain factor per unit length and $\kappa = \Delta\beta + 2\gamma P$ is the phase mismatch that combines the dispersion-induced linear phase shift $\Delta\beta$ expressed in Eq. (23)

with the nonlinear phase shift due to XPM. Note that the parametric gain factor g can be mathematically linked to the MI gain given in Eq. (18). Equation (24) shows that the parametric gain band can be easily tailored by dispersion management, especially by tuning the second and fourth-order dispersion coefficients of DSFs. Figure 3.10 shows a typical example of a flat parametric gain band of up to 100 nm that can be generated in a dispersion-tailored fiber arrangement.

7.3 Applications of Fiber OPA

Fiber-optic parametric amplifiers (FOPAs) and wavelength converters show a number of characteristics attractive to all-optical signal processing and ultra-high bit rate communication systems [28]. Their advantages over rare-earth-doped (Erbium) fiber amplifiers include a broad gain bandwidth and access to arbitrary wavelength ranges (by tailoring the fiber dispersion). They additionally offer the possibilities to achieve wavelength conversion and, as recently demonstrated, many other applications such as ultrafast all-optical signal sampling, limiting, buffering, high-repetition-rate pulse train generation, or time-division multiplexing [26][28]. In addition to broadband operation and high gain, FOPAs also provide low noise figures, equivalent to those of conventional optical fiber amplifiers or even better when they operate in a phase-sensitive configuration. First attempts were made in the 70's in the visible spectral region by use of birefringent or multimode fibers [23], and later in the 1.3 μm window with SMF [29]. Nowadays, most FOPAs are being developed in the 1.55 μm band to meet the requirements of the telecommunication industry [24].

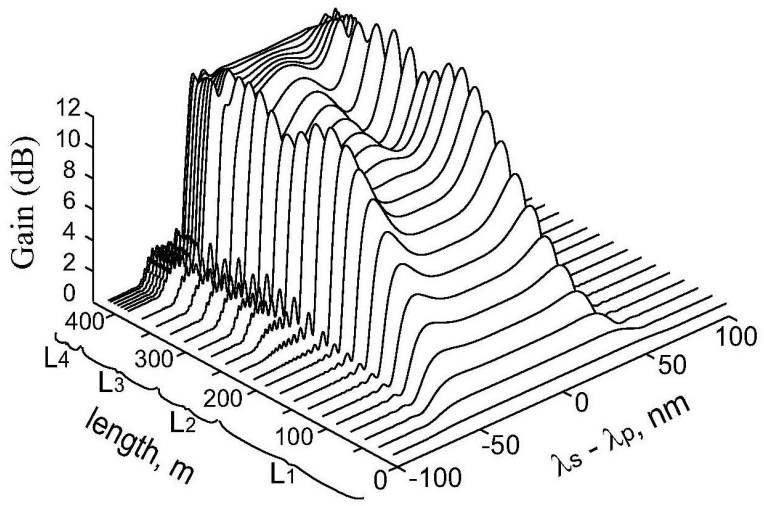

Figure 10 : Broadband and flat parametric gain versus pump-signal wavelength detuning in a dispersion-tailored four fiber arrangement obtained from a numerical simulation of Eq. (14) at P= 500 mW.

As many other nonlinear effects, Fiber OPA is strongly polarization-dependent. Therefore, the input state of polarization (SOP) of the signal must be parallel to that of the pump. The polarization dependence of the parametric gain can however be significantly reduced by using techniques such as polarization diversity or cross-polarized pump waves [26].

8. Stimulated Raman scattering (SRS)

8.1 Principle of Raman scattering

The principle of Raman scattering is schematically described in Fig. 3.11. This third-order nonlinear effect is an inelastic scattering process, where an incoming photon of energy $h\nu_i$ interacts with a coherently-excited state of the system E_v, that is, the vibrational modes of a silica (SiO_2) molecule. As a result of this light-matter interaction, a frequency down-converted photon $h\nu_s$ is emitted. The incident photons are annihilated to create a lower energy Stokes photon. Different to acoustic phonons, an optical phonon vibrating in the THz range involved in stimulated Brillouin scattering (SBS). Up-converted (anti-Stokes) photons may also be emitted if the excited state is sufficiently populated. The Raman effect was discovered by C. V. Raman in 1928 in liquids, for which he received

the Nobel Prize in Physics in 1930 [30]. What he observed was the spontaneous Raman scattering, in which an infinitesimal fraction (less than 10^{-6}) of the input energy is converted to the scattered light [31]. This effect does not provide optical amplification. However, if the incident laser beam is sufficiently intense, the photon-phonon scattering process becomes self-stimulated. The temporal beating between the pump and Stokes waves stimulates the vibrational states of silica molecules, and the wave grows rapidly as more and more pump energy is transferred to it. In the stimulated regime, the growth of the Stokes signal is exponential and much more efficient than in the anti-Stokes scattering which requires phonon population.

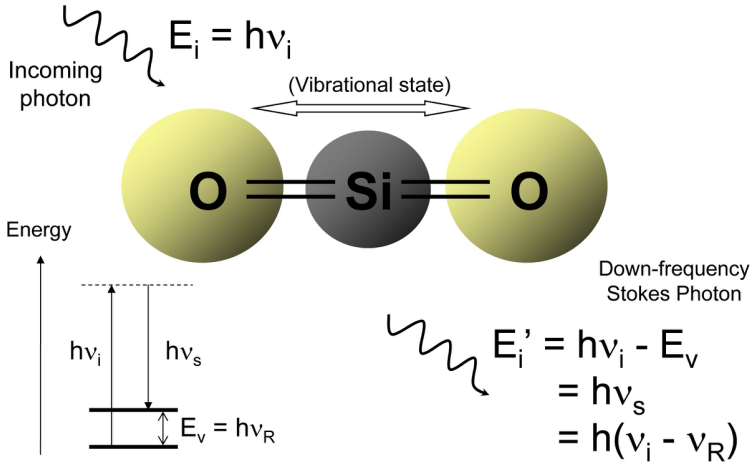

Figure 11 Principle of inelastic Raman scattering of light.

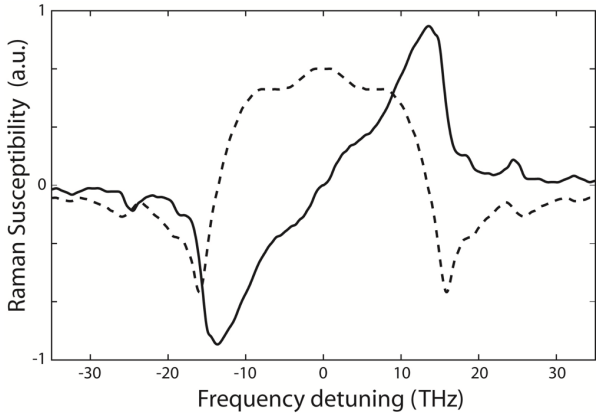

Figure 12 : Raman susceptibility in fused silica versus frequency detuning between pump and Stokes waves. Solid line: imaginary part. Dashed line: real part.

The Raman susceptibility $\chi_R^{(3)}(\omega)$, which is plotted in Figure 3.12, is the Fourier transform of the delayed Raman response $R(\tau)$ of Eq. (15) [32]. It exhibits a real part (dashed) and an imaginary part (solid curve) that are the Raman contribution to the Kerr effect and the Raman gain, respectively. This results from the Kramers-Kronig relations due to causality. This implies that the real part is a symmetric function whereas the imaginary part is anti-symmetric, with gain on the Stokes side and loss on the anti-Stokes side. Thus, in the stimulated regime, the anti-Stokes wave is absorbed by the pump through Raman scattering. In optical fibers, however, Raman anti-Stokes wave is often emitted via four wave-mixing [32]. The Raman frequency shift in fused silica is $\Omega_R/2\pi$=13.2 THz (440 cm^{-1}), which corresponds to the inverse of the fast response time of molecular vibrations (τ_R=75 fs) [34].

In the continuous-wave pumping regime, the nonlinear interaction between the pump and signal is governed by the following set of coupled power equations [4] :

$$\frac{\partial P_P}{\partial z} = -\frac{\omega_P}{\omega_S}\frac{g_R}{A_{eff}} P_P P_S - \alpha_P P_P \tag{24}$$

$$\frac{\partial P_S}{\partial z} = \frac{g_R}{A_{eff}} P_P P_S - \alpha_S P_S \tag{25}$$

where α_P and α_S are the absorption coefficients that are related to fiber loss at the pump and signal wavelengths. Equation (24) is readily solved if we neglect the first term of the right-hand side that accounts pump depletion. By substituting the solution in the second equation (25), we can easily solve the signal power at the amplifier's output:

$$P_S(L) = P_S(0)\exp\left(\frac{g_R}{A_{eff}} P_P L_{eff} - \alpha_S L\right) \tag{26}$$

with $P_S(0)$ and P_P, the input signal and pump power, respectively. A_{eff} is the fiber effective core area defined in Equation (7). g_R is the Raman gain coefficient which is typically of the order of 10^{-13} m/W in pure silica fiber. L_{eff} is the effective fiber length defined in equation (9).

Another important parameter to know is the Raman threshold or critical power. It is defined as the power for which the Stokes power generated from noise becomes equal to the pump power [4]:

$$P_{Th}(W) = \frac{16 A_{eff}}{g_R L_{eff}} \tag{27}$$

Note that the Raman gain efficiency g_R/A_{eff} can be significantly enhanced or frequency shifted by use of dopants inside the fiber core [35]. For instance, in fibers highly doped with germanium, the Raman gain can be seven times greater than that in SMFs. Two factors contribute to enhance the Raman gain in these fibers: first, the relatively high GeO_2 doping provides a larger Raman gain coefficient; second, the effective area can be made very small in these fibers, leading to higher power confinement and therefore larger gains. These fibers are often used in Raman amplifiers and lasers. In addition, phospho-silicate (P_2O_5) glass has two scattering bands shifted from 19.5 THz (650 cm^{-1}) and 39 THz (1300 cm^{-1}).

8.2 Raman amplifiers for telecommunications

Because of the amorphous nature of fused silica and the short phonon lifetime (τ_L=150 fs), optical fibers are used in a broadband gain process via Raman effect as shown in Figure 3.12. This wide gain bandwidth is very advantageous to make Raman fiber amplifiers (RFA) and Raman fiber lasers (RFL) [35]. For a pump at 1450 nm, the gain band provides maximum gain at 1550nm over a range of 40 nm as shown in figure 3.13.
Moreover, it is possible to generate a flat and wide gain bandwidth by injecting multiple pumps in a single optical fiber as shown in figure 3.14. Time-division multiplexing of pump wavelengths is often required to suppress energy transfer between the pumps in such a configuration. A wide gain bandwidth as shown in the figure has recently enabled to transmit data beyond 10 Tbit/s transfer rate over longer than 10000 km of fiber [33].

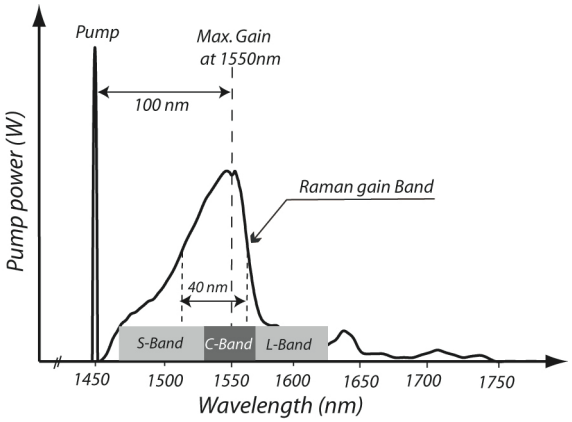

Figure 13 : Raman gain bandwidth at telecommunication wavelengths (S, C and L bands).

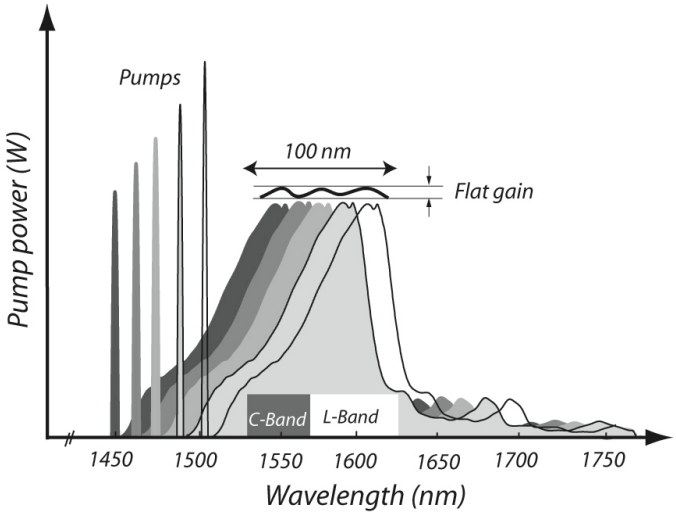

Figure 14 : Principle of multi-wavelength pumping for flat and broadband Raman amplification at telecommunication wavelengths (C and L bands).

Note also that Raman fiber amplification, like fiber OPA, is strongly polarization-dependent. The Raman gain coefficient of a signal with polarisation parallel to the pump is indeed 30 times higher than that of an orthogonally polarized one. However, by using cross-polarized pumps or pump polarization diversity, Raman gain independent on the polarization state of incident signal can be obtained.

8.2 Cascaded Raman generation

Cascaded Raman generation can be understood as an iteration of fundamental stimulated Raman scattering (SRS) processes. Stokes wave generated in each iteration acts as a pump to produce another Stokes wave with a different frequency. Cascaded SRS thus produces multiple additional lines or secondary radiations in the spectrum of light scattered in the optical fiber. As an example, Figure 3.14 shows cascaded Raman generation using a high-peak power 532-nm (green) nanosecond microchip laser and a 20-m long single-mode polarization maintaining fiber. Seven Raman orders can be seen from the green to the red as shown in the figure. Note that, in optical fibers, higher-order Stokes waves can often be obtained by four-wave mixing.

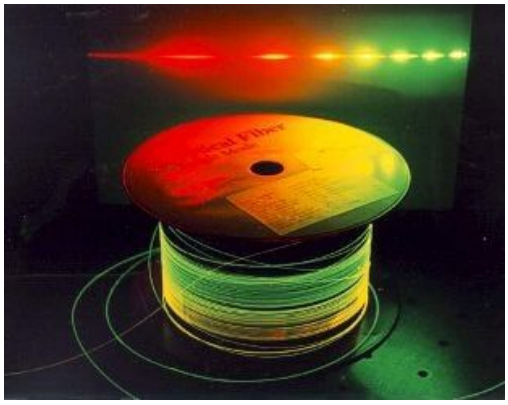

Figure 14 : The image shows cascaded Raman scattering by launching a 532-nm (green) nanosecond microchip laser into a 20m long single-mode polarization maintaining fiber. More than seven Raman orders can be observed from the green (input laser wavelength) to the red.

8.3 Raman Fiber Laser (RFL)

Optical fiber waveguides have been early recognized as an ideal medium to achieve cascaded Raman wavelength conversion for a purpose in generating new laser wavelengths and developing wide-band optical amplifiers. GeO_2 and P_2O_5 doped fibers are used extensively to construct Raman fiber lasers (RFLs), which can cover the whole spectral range from 1.2 μm to 2 μm [5]. The great advantage of RFLs over other high-power sources (doped fiber, semiconductor lasers, etc) is that cascaded Raman order generation efficiently allows access to spectral ranges previously unattainable with other technologies. As shown in Figure 3.15, RFL is an all-fiber nested Fabry-Perot resonator with a highly-doped fiber as a Raman gain medium and fiber Bragg grating (FBG) reflectors. In such a resonator, a high-power Ytterbium continuous pump wave near 1100 nm is converted into a single or multiple high-power waves in the 1200–1600 nm range through cascaded Raman generation. Typically, RFLs emit CW and deliver medium power (1 to 50 W). They are used as a convenient laser source for pumping optical fiber amplifiers and some lasers.

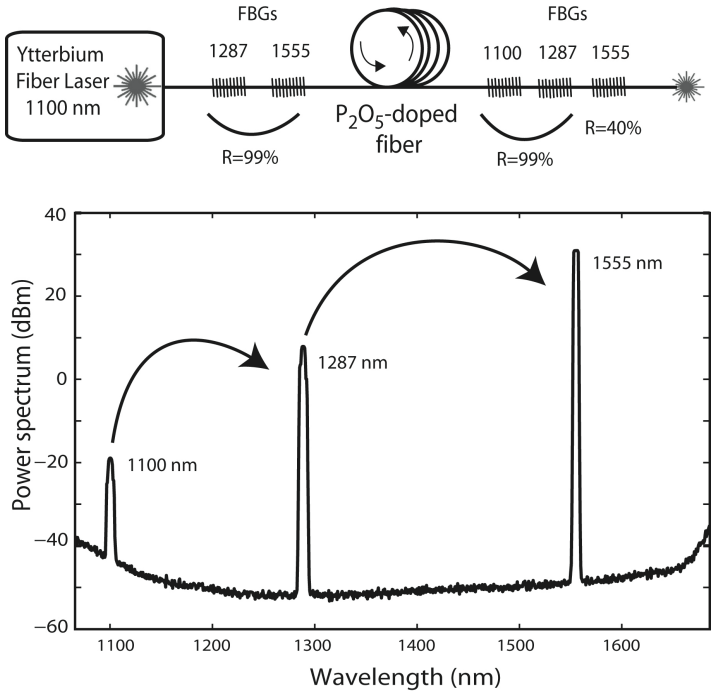

Figure 3.15 : Top : Setup of a dual-order cascaded Raman fiber laser made with a phosphosilicate fiber as Raman gain medium and five nested fiber Bragg gratings (FBGs) as reflectors. Bottom: RFL spectrum.

9. Conclusion

In this course, we have described the basics of all the nonlinear optical effects that occur when high-intensity electromagnetic fields propagate in optical fibers. As nonlinear fiber optics is a very attractive research field, it has been covered in many previous reviews and books. The readers are particularly recommended to refer to references [4] and [5] that combine both theory and experiments. Other books and references cited in the bibliography contain valuable material and handy references.

10. Bibliography

[1] N. Bloembergen, "Nonlinear optics: past, present and future," IEEE J Sel. Top. Quant., vol. 6, no. 6, pp. 876–880, 2000.

[2] R. W. Boyd, "Nonlinear optics," Academic Press, third edition, 2008.

[3] P. Mitra and J. Stark, "Nonlinear limits to the information capacity of optical fiberfiber communications", Nature, vol. 411, pp. 1027-1030, 2001.

[4] G. P. Agrawal "Nonlinear Fiber Optics," Academic Press, fourth edition, 2007.

[5] G. P. Agrawal, "Applications of Nonlinear Fiber Optics," Academic Press, Second edition, 2009.

[6] R. R. Alfano, "The supercontinuum laser source," Springer, 2006.

[7] D. A. Kleinman, "Nonlinear dielectric polarisation in optical media," Phys. Rev. 126, 1977-1979 (1962).

[8] P. V. Mamyshev and S. V. Chernikov, "Ultrashort pulse propagation in optical fibers," Opt. Lett. 15, 1076-1078 (1990).

[9] F. Shimizu, "Frequency broadening in liquids by a short light pulse," Phys. Rev. Lett. 19, 1097-1100 (1967).

[10] R. H. Stolen and C. Lin, "Self-phase modulation in silica optical fibers," Phys. Rev. A 17, 4, 1448–1453 (1978).

[11] N. J. Doran and D. Wood, "Nonlinear optical loop mirror," Opt. Lett. 13, pp. 56-58, 1988.

[12] S. Boscolo, S. K. Turitsyn, and V. K. Mezentsev, "Performance comparison of 2R and 3R optical regeneration schemes at 40 Gb/s for application to all-optical networks," J. Lightwave Technol. 23, 304–309 (2005).

[13] H. Sotobayashi, C. Sawaguchi, Y. Koyamada, and W. Chujo, "Ultrafast walk-off-free nonlinear optical loop mirror by a simplified configuration for 320-Gbit s time-division multiplexing signal demultiplexing," Opt. Lett. 27, 1555–1557 (2002).

[14] J. D. Moores, K. Bergman, H. A. Haus, and E. P. Ippen, "Optical switching using fiber ring reflectors," J. Opt. Soc. Am. B 8, 594–601 (1991).

[15] G. P. Agrawal and Y. S. Kivshar, "Optical Solitons: From Fibers to Photonic Crystals," Academic press (2003).

[16] A. Hasegawa and F. Tappert, "Transmission of stationary nonlinear optical pulses in dispersive dielectric fibers. I. Anomalous dispersion," Appl. Phys. Lett., vol. 23, no. 3, 142–144, (1973).

[17] P. Beaud, W. Hodel, B. Zysset, and H. P. Weber, "Ultrashort pulse propagation, pulse breakup, and fundamental soliton formation in a single-mode optical fiber," IEEE J. Quantum Electron., vol. 23, pp. 1938–1946, (1987).

[18] J. M. Dudley, G. Genty and S. Coen, "Supercontinuum generation in photonic crystal fiber," Rev. Mod. Phys. Vol. 78, 1135–1184 (2006).

[19] L. F. Mollenauer, R. H. Stolen, and J. P. Gordon, "Experimental observation of picosecond pulse narrowing and solitons in optical fibers," Phys. Rev. Lett., vol. 45, no. 13, 1095–1098 (1980).

[20] L. F. Mollenauer, M. J. Neubelt, J. S. G. Evangelides, J. P. Gordon, J. R. Simpson, and L. G. Cohen, Experimental study of soliton transmission over more than 10,000 km in dispersion-shifted fiber, Opt. Lett., vol. 15, 1203-1205 (1989).

[21] K. Smith and L. F. Mollenauer, "Experimental observation of adiabatic compression and expansion of soliton pulses over long fiber paths," Opt. Lett., vol. 14, no. 14, 751–753 (1989).

[22] A. Hasegawa and W. F. Brinkman, "Tunable coherent IR and FIR sources utilizing modulation instability," IEEE J. Quantum Electron. 16, 694-697 (1980).

[23] R. H. Stolen, "Phase-matched stimulated four-photon mixing in silica-fiber waveguides," IEEE. J. Quantum Electron. Vol. 11, 100-103 (1975).

[24] K. Hill, D. Johnson, B. Kawasaki, and R. MacDonald, "CW three-wave mixing in single-mode optical fibers," J. Applied Physics, vol. 49, 5098-5106 (1978).

[25] K. Inoue, "Four-wave mixing in an optical fiber in the zero-dispersion wavelength region", IEEE J. of Lightwave Technol., vol. 10, pp. 1553-1562 (1992).

[26] M. E. Marhic, "Fiber Optical Parametric Amplifiers, Oscillators and Related Devices," Cambridge University Press, Cambridge (2007).

[27] R. Stolen and J. Bjorkholm, "Parametric amplification and frequency conversion in optical fibers," IEEE J. Quant. Electron. 18, 1062–1072 (1982).

[28] J. Hansryd, P. A. Andrekson, M. Westlund, J. Lie, and P.-O. Hedekvist, "Fiber-based optical parametric amplifiers and their applications," IEEE. J. Sel. Top. Quantum Electron. Vol. 8, 506–520 (2002).

[29] J. P. Pocholle, J. Raffy, M. Papuchon, and E. Desurvire, "Raman and four-photon mixing amplification in single mode fibers," Opt. Eng. 24, 600-608 (1985).

[30] C.V Raman and K. S. Krishnan, "A new type of secondary radiation," Nature 1121, 501 (1928).

[31] R. W. Hellwarth, "Third-order optical susceptibilities of liquids and solids," Prog. Quant. Electr. 5, 1-68, (1977).

[32] R. H. Stolen and E. P. Ippen, "Raman gain in glass optical waveguides," Appl. Phys. Lett., vol. 22, no. 6, 276–278 (1973).

[33] N. Bloembergen and Y. R. Shen, "Theory of stimulated Brillouin and Raman scattering," Phys. Rev. 137, 6A, 1787–1805 (1965).

[34] R. H. Stolen, J. P. Gordon, W. J. Tomlinson, and H. A. Haus, "Raman response function of silica-core fibers," J. Opt. Soc. Am. B vol. 6, 1159–1166 (1989).

[35] M. N. Islam, "Raman Amplifiers for telecommunications 1: Physical Principles," Springer, (2004).